

LncRNA XLOC_015548 affects the proliferation and differentiation of myoblasts via the MAPK signaling pathway

Yihao Wei^{1,2,3*} , Tiantian Qi^{1,2*}, Siyang Cao^{1,2}, Weifei Zhang^{1,2}, Fei Yu^{1,2}, Hui Zeng^{1,2*} and Jian Weng^{1,2*}

¹Department of Bone & Joint Surgery, Peking University Shenzhen Hospital, Shenzhen 518036, China; ²National & Local Joint Engineering Research Center of Orthopaedic Biomaterials, Peking University Shenzhen Hospital, Shenzhen 518036, China;

³Shantou University Medical College, Shantou 515000, China

*These authors contributed equally to this paper.

Corresponding authors: Jian Weng. Email: jweng@pku.edu.cn; Hui Zeng. Email: zenghui_36@163.com

Impact Statement

For the first time, we have provided a complete and exhaustive study of the proliferation and differentiation of myoblasts affected by long non-coding RNA (lncRNA) XLOC_015548 in this article. We have reported related mechanisms (e.g. MAPK pathways, effects of proliferation and differentiation of myoblasts, and forming myotubes) and found that the expression of phosphorylated proteins of MEK/ERK was comparable to that of cells treated with MEK-specific inhibitors. We have also discussed in depth the promising prospect of targeting lncRNA XLOC_015548 in anti-disuse muscle atrophy therapy.

Abstract

In recent years, an increasing number of studies have reported that long non-coding RNAs (lncRNAs) play essential regulatory roles in myogenic differentiation. In this study, a specific lncRNA XLOC_015548 (Lnc000280) was identified. However, little research has explored its mechanism of action by constructing XLOC_015548 gene editing cell models. In this study, relevant sequences were obtained according to the RNA-seq results. Subsequently, XLOC_015548 knockdown and over-expression lentiviral vectors were constructed, and the C2C12 myoblast cell line was transfected to prepare the XLOC_015548 gene-edited myoblast model. The *in vitro* analysis revealed that over-expression of XLOC_015548 significantly promoted the proliferation and differentiation of myoblasts and the formation of myotubes, whereas the opposite result was obtained in the knockdown group. XLOC_015548 regulated myogenic differentiation and affected the expression of myogenic differentiation regulators such as Myod, myogenin, and MyHC. Regarding the signaling pathway, we found that XLOC_015548 correlated with the phosphorylation level of MAPK/MEK/ERK pathway proteins. And the degree of phosphorylation was positively

correlated with the protein expression of myogenic differentiation regulators. In conclusion, a new gene-edited myoblast model was constructed based on the lncRNA regulator XLOC_015548. The *in vitro* cell experiments verified that XLOC_015548 had regulatory effects on muscle growth and myoblast differentiation. These findings provide a laboratory foundation for the clinical application of lncRNAs as regulatory factors in the treatment of disuse muscle atrophy.

Keywords: Long non-coding RNA XLOC_015548, myoblast differentiation, myogenesis, MAPK signaling pathway, RNA sequencing, muscle

Experimental Biology and Medicine 2023; 248: 469–480. DOI: 10.1177/15353702231151963

Introduction

As one of the most abundant tissues in organisms, the skeletal muscle is mainly responsible for maintaining movement and shape and performing secretory functions.^{1,2} The typical structural and functional integrity of skeletal muscles correlates with innervation, nerve conduction, nerve impulses, and metabolic processes within muscle cells.^{3,4} Accumulating evidence shows that the damage or poor development of skeletal muscles is associated with various disease states, including denervation-induced muscle

atrophy, cancer cachexia, endocrine dysfunction, and metabolic diseases.^{5–8} The skeletal muscle can be generated via a multistep and complex process, including myogenic precursor recruitment, cell proliferation, cell fusion, and myotube differentiation.^{9–11} Existing studies show that the generation of skeletal muscles is related to the transcription and expression of myogenic regulator factors (MRFs) at the epigenetic level.¹² For instance, myogenic differentiation factor (MyoD), myogenin (Myog), and myogenic regulatory factor 4 (MRF-4) play crucial roles in the processes of myogenesis and muscle differentiation.^{13–15} Therefore, exploring the regulatory

effects of myogenic regulators is of great significance to protect the remaining muscles and alleviate muscle atrophy after skeletal muscle injuries.

Abundant epigenetic studies have confirmed the presence of various non-coding RNAs (ncRNAs) in skeletal muscles, including long non-coding RNAs (lncRNAs) with a length of more than 200bp, which are involved in the process of myogenic regulation and play crucial roles in muscle development.^{16,17} As the first muscle-specific lncRNA discovered, Linc-MD1 in the cytoplasm can positively regulate myogenic differentiation.¹⁸ Linc-YAM1, which is related to YY1, is a critical negative regulator of myogenesis and can be observed in the nucleus and cytoplasm of myogenic cells.¹⁹ The knockdown of YAM1 in C2C12 myocytes and myotubes could increase the number of multiple myogenic markers, and the downregulation of YAM1 could overcome the inhibitory effect of the transcription factor YY1 on myogenic differentiation.²⁰ Other lncRNAs, such as MUNC, can act as positive regulators of myogenesis and regulate myogenic differentiation through different mechanisms. They can directly upregulate the expression of endogenous muscle differentiation factors, including Myod, Myog, and Myh3 genes.²¹ Similarly, lncMyod, located upstream of the *MYOD1* gene, can promote myogenesis and muscle differentiation.²² These findings suggest that lncRNAs play essential roles in biological myogenesis. In summary, given the notable regulatory effect of lncRNAs on myogenesis, their use to regulate myogenic regulators and achieve the purpose of preserving muscles and alleviating muscle atrophy may be assumed.

Our research team construct a mouse model of denervation-induced gastrocnemius muscle atrophy after peripheral nerve injuries and use RNA-seq technology to analyze the biological effect of ncRNAs on the transcriptome of skeletal muscle atrophy.²³ According to the expression difference and abundance, 73 lncRNAs are found to be statistically different in the process of muscle atrophy. Among them, XLOC_015548 (Lnc000280) shows the ideal expression abundance and the most significant expression difference as per the sequencing results (Supplementary File 1). XLOC_015548 is also subjected to pathway enrichment analysis through the KEGG database, and the results show that it is closely related to the mitogen-activated protein kinase (MAPK) signaling pathway (Supplementary Files 2–6). To our knowledge, no research has examined the correlation between XLOC_015548 and the MAPK pathway. Previous studies have revealed that MAPKs are a class of phosphatases widely distributed in tissues and encoded by mammalian genes, mainly through the dephosphorylation of threonine and tyrosine residues. Since the discovery of the MAPK family, researchers have carried out extensive explorations into the expression and function regulation of MAPKs in different cells, tissues, and organs. Among them, the extracellular signal-regulated kinase (ERK) is one of the most characteristic members of the MAPK family, and its functions are related to cell aging, apoptosis, proliferation, and differentiation.²⁴ The activation of ERKs is closely related to a major signaling axis of RAF-MEK-ERK.²⁵ In recent years, it has been demonstrated that ERK1/2 phosphorylation can upregulate the expression of Myod and promote the proliferation and differentiation of myoblasts.²⁶ Based on that, XLOC_015548 may be a key

target related to muscle atrophy and may regulate myogenic differentiation through the MAPK/Myod signaling pathway. Its specific effect is also under verification and exploration by our team. Therefore, this study was conducted to explore the effect of XLOC_015548 on myoblasts by inducing XLOC_015548 to infect C2C12 myoblasts *in vitro* with the assistance of lentiviral vector technology.

Materials and methods

C2C12 cell culture and U0126 treatment

The mouse myoblast cell line C2C12 (Procell Life Science & Technology Co., Ltd., Wuhan, China) was routinely resuscitated and inoculated in a 10-cm petri dish. The cells proliferated in the complete culture medium of 10% fetal bovine serum (VOLUME fraction) + 1% streptomycin and penicillin + DMEM (Dulbecco's Modified Eagle Medium). Subsequently, the cells were cultured in a cell incubator with 5% CO₂ (volume fraction) at 37°C, and the medium was replaced every 48h. When the degree of cell proliferation and fusion reached about 80%, the cells were cultured at a ratio of 1:3. Next, the cultured C2C12 cells continued to proliferate and were cultured under the same conditions. To induce C2C12 myoblasts to differentiate into myotubes, when the cell fusion reached 50–60%, the complete medium was discarded and replaced with differentiation containing 2% horse serum + 1% streptomycin and penicillin + high-glucose DMEM culture medium. The medium was replaced every 24h for 6 days to induce differentiation. According to the manufacturer's instructions, 1 μg/mL U0126 was prepared to maintain the concentration for 48h. After the above treatment, the residual agent was removed by routinely rinsing the cells with phosphate-buffered saline (PBS) two to three times.

Construction and transfection of the XLOC_015548 over-expression and knockdown lentiviral vector system

Lentiviruses were designed according to the gene sequence of XLOC_015548.²³ The viral vector HBLV-m-Lnc000280-shRNA1-ZsGreen-PURO was constructed with the pHBLV-U6-MCS-CMV-ZsGreen-PGK-PURO interference vector. The HBLV-m-Lnc000280-Null-ZsGreen-PURO over-expression vector was constructed with the pHBLV-CMV-MCS-EF1-ZsGreen-T2A-puro vector. Subsequently, the primers were annealed with two restriction enzyme sites, namely, BamH I and EcoR I, to synthesize double-stranded DNA. Then, T4 DNA ligase was used to transform the double-digested vector and the annealed double-stranded DNA into competent cells. Next, the positive clones were identified with polymerase chain reaction (PCR). After sequencing, the plasmid was extracted for subsequent experiments after identification. After 293T cells were transfected for 5 days, the fluorescence cells in the diluent of each virus were observed under a fluorescence microscope. The packaged lentiviral particles were collected as per titer (TU/mL) = number of cells × percentage of positive clones × multiplicity of infection (MOI) × virus dilution × 10³ TU/mL. The C2C12 cells were divided into the negative control group, the XLOC_015548 knockdown

group, the positive control group, and the XLOC_015548 over-expression group. After that the cells were transfected with an MOI of 20 \times . After 12–24 h of incubation, the proliferation medium was replaced, and the first passage was carried out after 72 h of culture. Then, 2 mg/mL puromycin was added to select stable transfectants. After 72 h, the cells were photographed under a fluorescence microscope and collected for subsequent experiments.

Green fluorescent protein

To identify whether the target cells could be successfully transfected with the XLOC_015548 over-expression and knockdown lentiviral vector system, the expression of green fluorescent protein (GFP) in cells transfected with lentiviruses for 24–96 h was observed using fluorescence microscopy.

Cell proliferation assay (EdU)

After being transfected with knockdown empty lentiviruses, XLOC_015548 knockdown lentiviruses, over-expressed empty lentiviruses, and XLOC_015548-over-expressed lentiviruses, the cells in each group were inoculated in six-well plates (5000 cells/well). The EdU solution (C10310-3 kit; RIBBIO, Guangzhou, China) was added to the plate and incubated for 12 h, followed by fixation and other treatment procedures. The cells were then stained with DAPI and observed with fluorescence microscopy.

Calcein-AM/PI staining experiment

The cells were inoculated in 96-well plates at a density of 3×10^4 cells per well in an incubator with 5% CO₂ at 37°C. After 24 h of incubation, the culture medium was drawn and washed with PBS two to three times. According to the manufacturer's instructions, the viability of cells was detected with the Calcein/PI Cell Viability/Cytotoxicity Assay Kit (Beyotime; Cat: C2015M, Shanghai, China). Subsequently, the cells were observed and photographed under an inverted fluorescence microscope, and the survival rate was calculated as per the following formula: cell survival rate (%) = (Calcein-AM + cell number) / (Calcein-AM + cell number + PI + cell number) \times 100%.

Cell Counting Kit-8 assay

After being transfected with small interfering RNA (siRNA), the cells were first seeded into 96-well culture plates at 5×10^3 cells per well and then incubated for 24, 48, and 72 h. Cell Counting Kit-8 (CCK-8) solution (Beyotime; Cat: C0038) 10 μ L/well was added and cultured in an incubator for 1 h. The absorbance of each well at a wavelength of 450 nm was measured with a plate reader to reflect the cell proliferation activity.

Myotube contractility test

According to a previous study, cell contractility can be quantified using carbachol to stimulate muscle cells and continuously capture cell images at intervals.²⁷ After being treated with the differentiation medium for 6 days, the cells were stimulated with 200 μ M carbachol (Macklin, C13124182, carbamylcholine chloride). Five high-quality images of the cells were taken consecutively at 2-min intervals during

carbachol stimulation. The difference in integrated optical density (IOD) of the first and subsequent images was mainly caused by myotube contractions. Therefore, the average IOD of the differential image can be used to represent the contraction index (i.e. contraction index = $(\sum(|\text{IOD}_5 - \text{IOD}_4| + |\text{IOD}_4 - \text{IOD}_3| + |\text{IOD}_3 - \text{IOD}_2| + |\text{IOD}_2 - \text{IOD}_1|))/4$). In the formula, IOD1 to IOD5 represent the average IOD values of the first to fifth images, respectively. IODs were analyzed with Image-Pro Plus (Media Cybernetics, Rockville, MD, USA).

Immunofluorescence

The cells were fixed in 4% paraformaldehyde for 15 min and permeabilized with 0.5% Triton X-100 for 15 min at room temperature. Then, they were blocked with 5% bovine serum albumin (BSA) for 30 min at room temperature and incubated overnight with anti-myosin heavy chain (MyHC) primary antibodies (Invitrogen, PA5-31466, 1:50, Waltham, MA, USA) at 4°C with gentle shaking. After being washed three times with PBS for 10 min, the cells were exposed to secondary antibodies (CST, 1:100). The nuclei were counter-labeled with DAPI. Immunofluorescence images were displayed on a fluorescence microscope (Q500MC; Leica Image Analysis System, Germany).

SiRNA transfection

The C2C12 cells were seeded at a density of 5×10^5 cells per well of six-well plates. Cells were transfected with siRNA targeting mouse XLOC_015548 or with negative control siRNA (GenePharma, Shanghai, China) using the Lipofectamine 3000 reagent (Invitrogen) based on kit instructions and incubated for 12 h. Knockdown efficiency was determined using quantitative polymerase chain reaction. The sequences of the siRNAs targeting XLOC_015548 were as follows: siRNA#1 sense, 5'-GCAUUUGAACCCUUUCAATT dTdT-3'; antisense, 3'-dTdT UUUGAAAGGGUUCAAAUGCTT-5'. siRNA#2 sense, 5'-GCCCCUUGUCAUUUAGCUAATT dTdT-3'; antisense, 3'-dTdT UUAGCUAAAUGACAAGGGCTT-5'. siRNA#3 sense, 5'-GCAUGGCCAUAAUGACAATT dTdT-3'; antisense, 3'-dTdT UUGUCAUUAUGGACCAUGCTT-5'.

Real-time quantitative PCR (RT-qPCR)

After being treated with the differentiation medium for 3 days, the total RNA was isolated with RL solution reagents (Beibei Biotechnology Co., Ltd., Hebei, China). According to the experimental procedure, 1 μ g RNA was reversely transcribed with the PrimeScript RT Kit (Takara, Liaoning, China). The synthesized cDNA (complementary DNA) was diluted at a dilution of 1:5, and then reverse transcription-quantitative polymerase chain reaction (RT-qPCR) was performed with a fast real-time PCR system. The relative abundance of RNA was determined using SYBR PreMix Ex Taq II (Takara) and the LightCycler480PCR system according to the manufacturer's instructions. The temperature was set as follows: 95°C for 30 s, followed by 40 cycles of 95°C for 5 s and 60°C for 30 s. Each RT-qPCR was performed in a 10 μ L reaction mixture. The primer sequences were as follows: for GAPDH, 5'-AGGTCGGTGTGAACGGATTTG-3' (forward) and 5'-GGGGTCTTGATGGCAACA-3' (reverse); for Myod, 5'-GCTCTGATGGCATGATGGATT-3' (forward)

and 5'-GCGGTGTCGTAGCCATTCT-3' (reverse); and for XLOC_015548, 5'-CCTCAGCAGACCCTGACTGTAG-3' (forward) and 5'-CAGTGGCTGTCTTAGTCCATCTCA-3' (reverse).

Western blot analysis

After being treated with the differentiation medium for 6 days, the cells were prepared with lysis buffer (Beyotime). After the protease inhibitors and phosphatase inhibitors were supplemented, the cells were sonicated and centrifuged at 12,000g and 4°C for 30 min. The supernatant was collected, and protein quantification was performed using the bicinchoninic acid (BCA) assay. According to different groups, 35 µg protein was separated on 10% SDS-PAGE (sodium dodecyl sulfate-polyacrylamide gel electrophoresis) gel and transferred to polyvinylidene difluoride membranes. The membranes were blocked with 5% BSA in Tris-buffered saline with Tween (TBST) for 45–90 min on a low-speed shaker. Then, they were incubated overnight with Myod1 antibodies (ABclonal; A0671, 1:1000, Wuhan, China), MEK1/2 antibodies (Abcam; ab178876, 1:1000, Cambridge, MA, USA), p-MEK1/2 antibodies (Abcam; ab278723, 1:1000, Cambridge, MA, USA), ERK1/2 antibodies (Abcam; ab32537, 1:1000, Cambridge, MA, USA), p-ERK1/2 antibodies (CST, 5683, 1:1000, Danvers, MA, USA), myogenin antibodies (Abcam; ab124800, 1:1000, Cambridge, MA, USA), Myosin Heavy Chain 1 (MYH1) antibodies (Thermo Fisher Scientific; PA5-31466, 1:1000, MA, USA), vinculin antibodies (Fine Biotech; FNab09799, 1:1000, Wuhan, China), and β-actin antibodies (ABclonal; A2319, 1:5000, Wuhan, China) at 4°C. The next day, they were incubated with horseradish peroxidase-conjugated secondary antibodies at room temperature for 1 h. The protein bands were detected with the ECL Hypersensitive Chemiluminescence Substrate Kit (Biosharp Biotechnology Co., Ltd., Beijing, China).

Statistical analysis

SPSS 21.0 was used to perform the statistical analysis, and Graphpad Prism 9.0 was used for image production. All data were analyzed with a *t*-test, and the results were expressed as mean ± standard deviation. $P < 0.05$ indicated that the difference is statistically significant.

Results

Construction of the XLOC_015548 gene editing cell model

After lentiviral transfection, the GFP level was determined from 24 to 96 h. There was a significant expression of GFP in the knockdown empty control group, the XLOC_015548 knockdown lentivirus group, the over-expression empty control group, and the XLOC_015548 over-expression lentivirus group (Figure 1(A)). In addition, RT-qPCR was performed to evaluate the mRNA expression level of XLOC_015548, as shown in Figure 1(B). Compared with the corresponding control groups, the XLOC_015548 knockdown group showed lower RNA expression levels, whereas the XLOC_015548 over-expression group showed high RNA expression levels in the cells ($P < 0.05$). Based on the above

observations, the target genes were successfully transfected into C2C12 myoblasts.

Detection of XLOC_015548 gene abundance and siRNA transfection efficiency

The C2C12 cells were transfected with XLOC_015548 siRNA#1, siRNA#2, siRNA#3 to downregulate the expression of the XLOC_015548 gene. The mRNA levels in the negative control siRNA and normal cell groups were significantly higher than those in the C2C12 cells transfected with XLOC_015548-siRNA (Figure 1(C)).

Effects of XLOC_015548 on cell viability and proliferation

To investigate the effect of XLOC_015548 on the viability and proliferation of C2C12 myoblasts, the live/dead cell double staining kit (Calcein-AM/PI) was used to detect apoptosis, and the EdU assay and CCK-8 were performed to measure cell proliferation. The results of Calcein-AM/PI staining showed that the over-expression of XLOC_015548 reduced the apoptosis of myoblasts, and these myoblasts had a higher survival rate compared with the negative control group (Supplementary File 7). The EdU assay results indicated that over-expression of XLOC_015548 promoted the proliferation of myoblasts. Compared with the negative control group, the knockdown of XLOC_015548 induced opposite results in terms of cell viability and proliferation (Figure 1(E) and Supplementary File 7) ($P < 0.05$). The CCK-8 results showed that after being transfected with XLOC_015548 siRNA, the growth rates of C2C12 cells slightly declined (Figure 1(F)).

Effects of XLOC_015548 on myotube activity and contractility

After the differentiation medium treatment for 6 days, C2C12 cells were fused to form typical multinucleated myotubes (Figure 2(A)). To further investigate the effect of XLOC_015548 on myotube formation during *in vitro* myogenesis, the number of myotubes was observed with fluorescence microscopy (Figure 2(B)). The results suggest that the knockdown of XLOC_015548 could significantly inhibit the differentiation of C2C12 cells, which can be manifested as the downregulated expression of MyHCs and a decrease in the number of positive myotubes. In addition, the over-expression of XLOC_015548 promoted the differentiation of C2C12 cells, increased MyHC immunostaining, and increased the number of myotubes (Figure 2(C) and (D)) ($P < 0.05$). To examine cell contractility, the cells were treated with 200 µM carbachol, and C2C12 myotubes contracted significantly (Figure 2(E)). The comparative analysis results indicated that C2C12 myotubes in the XLOC_015548 over-expression group exhibited more significant contractile activity, whereas those in the XLOC_015548 knockdown group showed opposite results (Figure 2(F) and (G)) ($P < 0.05$).

Positive effects of XLOC_015548 on myogenic differentiation

RT-qPCR was performed to determine the mRNA expression of Myod, a key factor in myogenic differentiation.

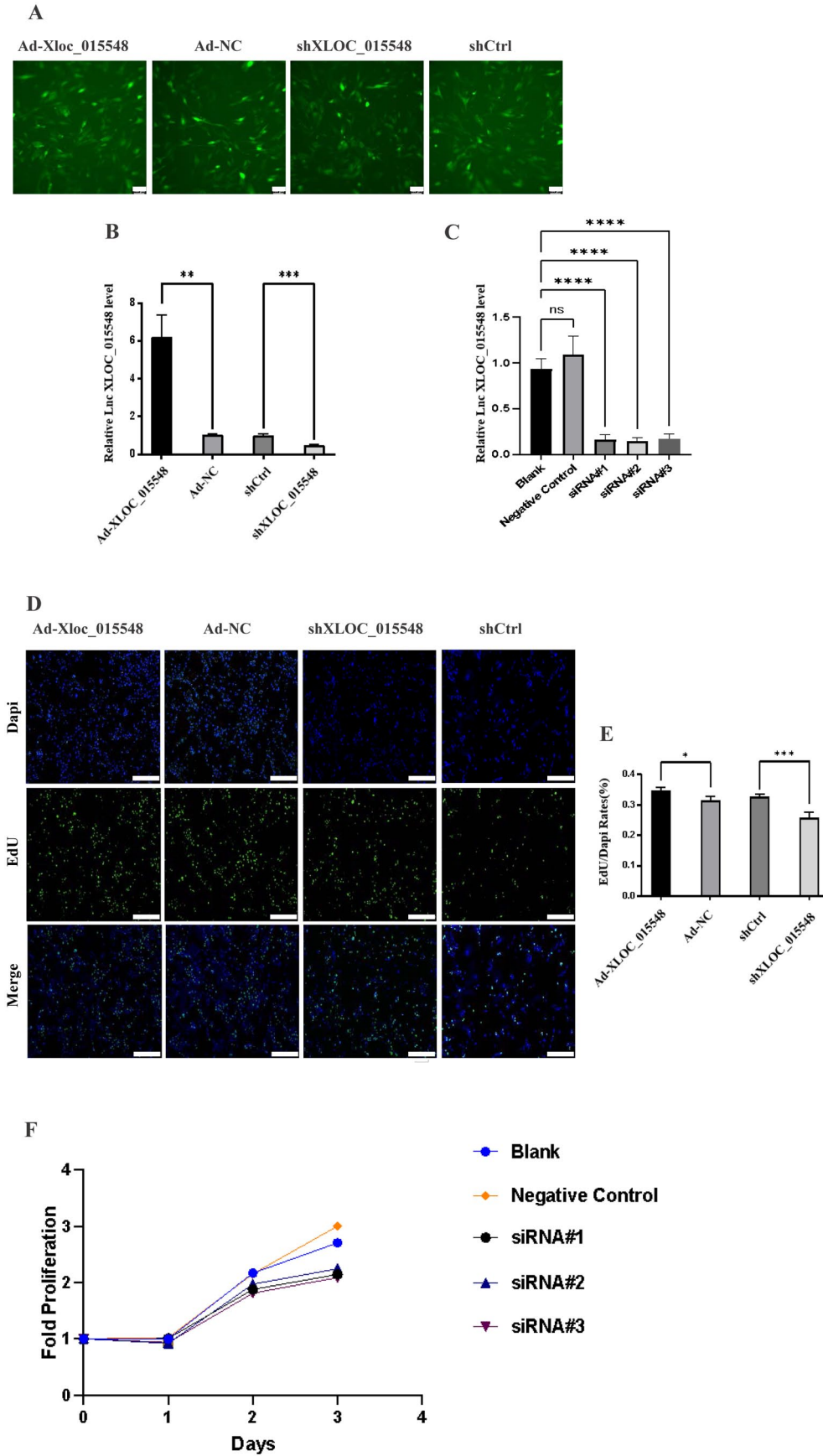


Figure 1. Construction of the XLOC_015548 gene editing cell model and the effect of XLOC_015548 on cell viability and proliferation. (A) After lentiviral transfection, the GFP level of the cells in each group was observed using a fluorescence microscope. (B, C) The mRNA expression of XLOC_015548 in each group was determined using RT-qPCR. (D, E) The EdU assay was performed to identify the survival rate and proliferation ability of the cells in each group after lentiviral transfection. (F) CCK-8 was used to detect the growth rates of C2C12 cells. Each experiment was repeated three times, and the data were expressed as mean \pm standard deviation. Scale bars, 100 μ m. * $P < 0.05$; ** $P < 0.01$.

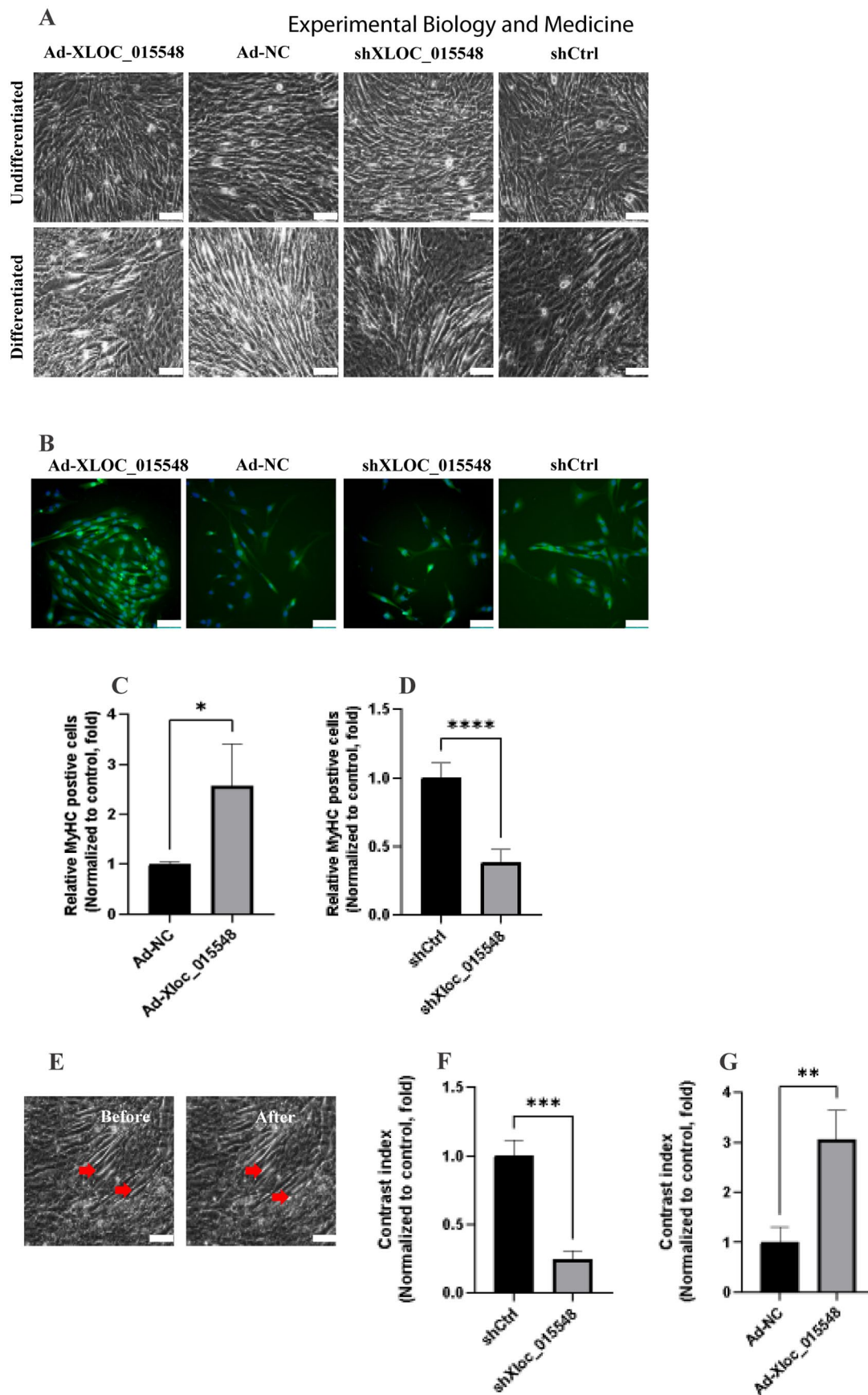


Figure 2. Effects of XLOC_015548 on myotube activity and contractility. (A) The differentiation medium promoted the fusion of cells in each group to form myotubes. (B–D) The immunofluorescence assay was used to detect the positive rate of MyHC in the myotubes after differentiation in each group. (E–G) The myotube contraction assay was performed to detect the contractility and activity of the myotubes. Each experiment was repeated three times, and the data were expressed as mean \pm standard deviation. Scale bars, 100 μ m. * P < 0.05; ** P < 0.01.

It was found that the mRNA expression of Myod was upregulated in the XLOC_015548 over-expression lentivirus group compared with the control group (Figure 3(G)), whereas the opposite result was obtained in the XLOC_015548 knockdown lentivirus group (Figure 3(A)) ($P < 0.05$). This suggests that XLOC_015548 may affect myocyte differentiation by upregulating the expression of Myod. To further explore the effect of XLOC_015548 on myogenic differentiation, western blot analysis was performed. The results were consistent with those of RT-qPCR (Figure 3(D) and (E)). XLOC_015548 can upregulate the expression of Myod mRNA and protein. Besides, in XLOC_015548-siRNA groups, we examined other myoblast-related proteins which saw a downtrend (Figure 4(A), (D) to (F)). Therefore, the expression level of XLOC_015548 played a positive role in myogenic differentiation (Figure 3(J) and (K)) ($P < 0.05$).

Effects of XLOC_015548 on promoting myogenic differentiation through phosphorylation of the MAPK signaling pathway

In the KEGG database, the pathway enrichment results indicated that XLOC_015548 was closely related to the MAPK signaling pathway. To explore the specific effect of XLOC_015548 on the MAPK signaling pathway, the expression of phosphorylated proteins of MEK1/2 and ERK1/2 in the MAPK pathway was detected (Figure 3(D) and (J)). The results indicated no significant difference in the total protein of MEK1/2 and ERK1/2 between the XLOC_015548 over-expression group and the control group. However, the expression of the phosphorylated protein of MEK1/2 and ERK1/2 showed an upward trend (Figure 3(B), (C), and (F)), whereas the opposite result was obtained in the XLOC_015548 knockdown group (Figure 3(H), (I), and (L)) ($P < 0.05$) and XLOC_015548-siRNA groups (Figure 4(A) to (C)). In addition, after U0126 treatment (Figure 4(G)), the expression of the phosphorylated protein of MEK1/2 and ERK1/2 in the XLOC_015548 knockdown group showed a downward trend compared with the control group without U0126 treatment (Figure 4(J) to (L), and the expression level of relevant proteins was similar to that of the control group with U0126 treatment ($P < 0.05$). It can also be found that the expression of Myod and Myog decreased in the XLOC_015548 knockdown group or the control group after U0126 treatment compared with the control group without U0126 treatment (Figure 4(H) and (I)) ($P < 0.05$). In the XLOC_015548 over-expression group treated with U0126, the expression of Myod was comparable to that in the control group ($P < 0.05$).

Discussion

Some studies show that three common factors can cause skeletal muscle atrophy: (1) chronic diseases, (2) disuse diseases (metabolism, denervation, and other conditions after fractures), and (3) sarcopenia. Although researchers have investigated skeletal muscle atrophy extensively, specific mechanisms remain unclear.^{28–31} Disuse skeletal muscle atrophy would undergo a process of chronic imbalance between the synthesis and breakdown of muscle proteins. Muscle atrophy gradually leads to a significant decline in skeletal

muscle mass and function by accelerating the protein degradation process, which, in turn, causes muscle fiber atrophy and loss. Some injuries or diseases often impose a phase of muscle disuse on the body, during which accelerated skeletal muscle atrophy and loss of functional strength can result in adverse consequences.³² Muscles, bones, and nerves are indispensable components of orthopedic diseases, and they play a central role in the prophylaxis and treatment of these diseases. Avoiding skeletal muscle atrophy, which is an important link in the rehabilitation of nerve and bone injuries, is significant. As demonstrated in numerous studies, the decline in skeletal muscle mass and function is prone to osteopenia, which, in turn, leads to osteoporosis. When skeletal muscle atrophy is accompanied by osteoporosis, there is an increased risk of falls, fractures, and even death. Meanwhile, the normal structure between muscle fibers and nerves in the neuromuscular system will also be destroyed in the pathological state of skeletal muscle atrophy. Therefore, after fracture healing and nerve repair, skeletal muscle atrophy will affect the quality of life and the effects of rehabilitation.^{33–35} Based on these, conducting further explorations into the pathogenesis of skeletal muscle atrophy for the clinical treatment of orthopedic diseases is necessary.

In skeletal muscle disuse diseases, taking denervated muscles as an example, the target muscles with damaged nerve endings will undergo structural, biochemical, and physiological changes, and about 80% of the muscle mass will be lost, which will eventually induce apoptosis and muscle atrophy. Over time, these muscles at nerve endings lose their receptivity to regenerated motor axons because of necrosis of muscle fibers, hyperplasia of connective tissue, concurrent failure of myocyte regeneration capacity, and massive loss of myocytes.^{36,37} In some studies, specific lncRNAs related to muscle differentiation have been identified through animal experiments. After Lnc-Mg is specifically knocked out in mice, the muscles of mice are atrophied, and exercise tolerance is lost. After the specific over-expression of Lnc-Mg, the muscles in mice become more hypertrophic.³⁸ In a previous study by our team, the atrophic gastrocnemius muscle of denervated mice was analyzed using the RNA-seq assay. A total of 73 differentially expressed lncRNAs were identified. Among these, a downregulated lncRNA XLOC_015548 was selected in the atrophic gastrocnemius muscle. However, there have been no reports on the effect of XLOC_015548 on myogenic differentiation. To verify whether XLOC_015548 can affect myogenic differentiation in muscle cells, the XLOC_015548 lentiviral vector was constructed in this study to conduct *in vitro* experiments.

For the first time, an XLOC_015548 gene editing cell model was successfully constructed in this study by transfecting XLOC_015548 knockdown and over-expression lentiviruses into myoblast C2C12 cells in an attempt to explore the effect of XLOC_015548 on myocyte proliferation and myoblast differentiation. Through the EdU assay and Calcein-AM/PI staining assay, we assume that XLOC_015548 increased the proliferation ability of C2C12. However, the ratio of dead cells to live cells of cells infected with XLOC_015548 lentivirus was low, indicating that the infection of XLOC_015548 lentivirus would not cause a large number of cell death and would not affect the biological activity of myoblasts.

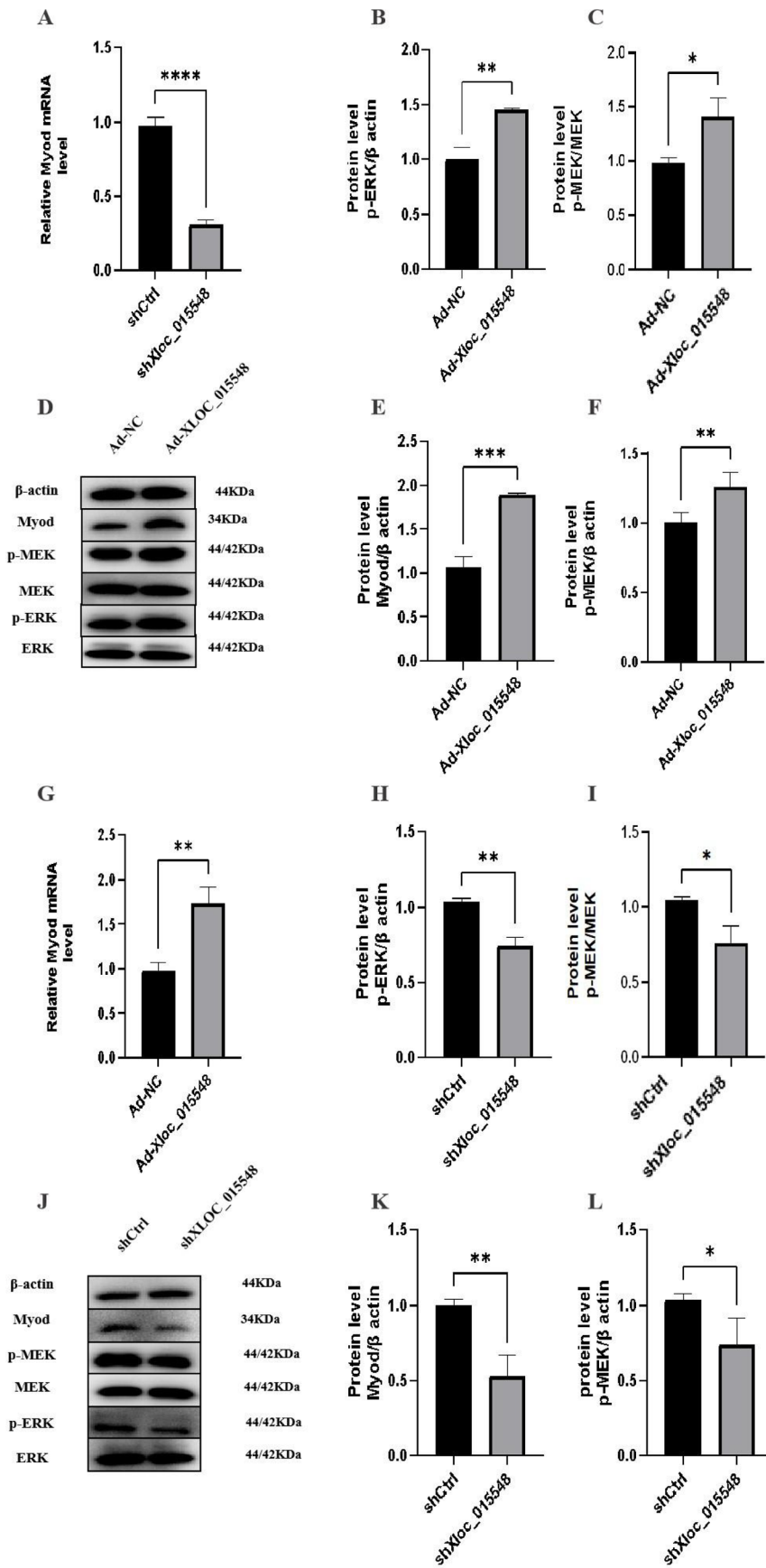


Figure 3. XLOC_015548 promoted the differentiation of myoblasts. (A, G) RT-qPCR was performed to determine the mRNA expression of Myod in each group. (B–D and H–I) Western blot analysis was conducted to identify the protein expression of Myod and MEK/ERK signaling pathway in lentivirus infection groups. Each experiment was repeated three times, and the data were expressed as mean \pm standard deviation. * $P < 0.05$; ** $P < 0.01$.

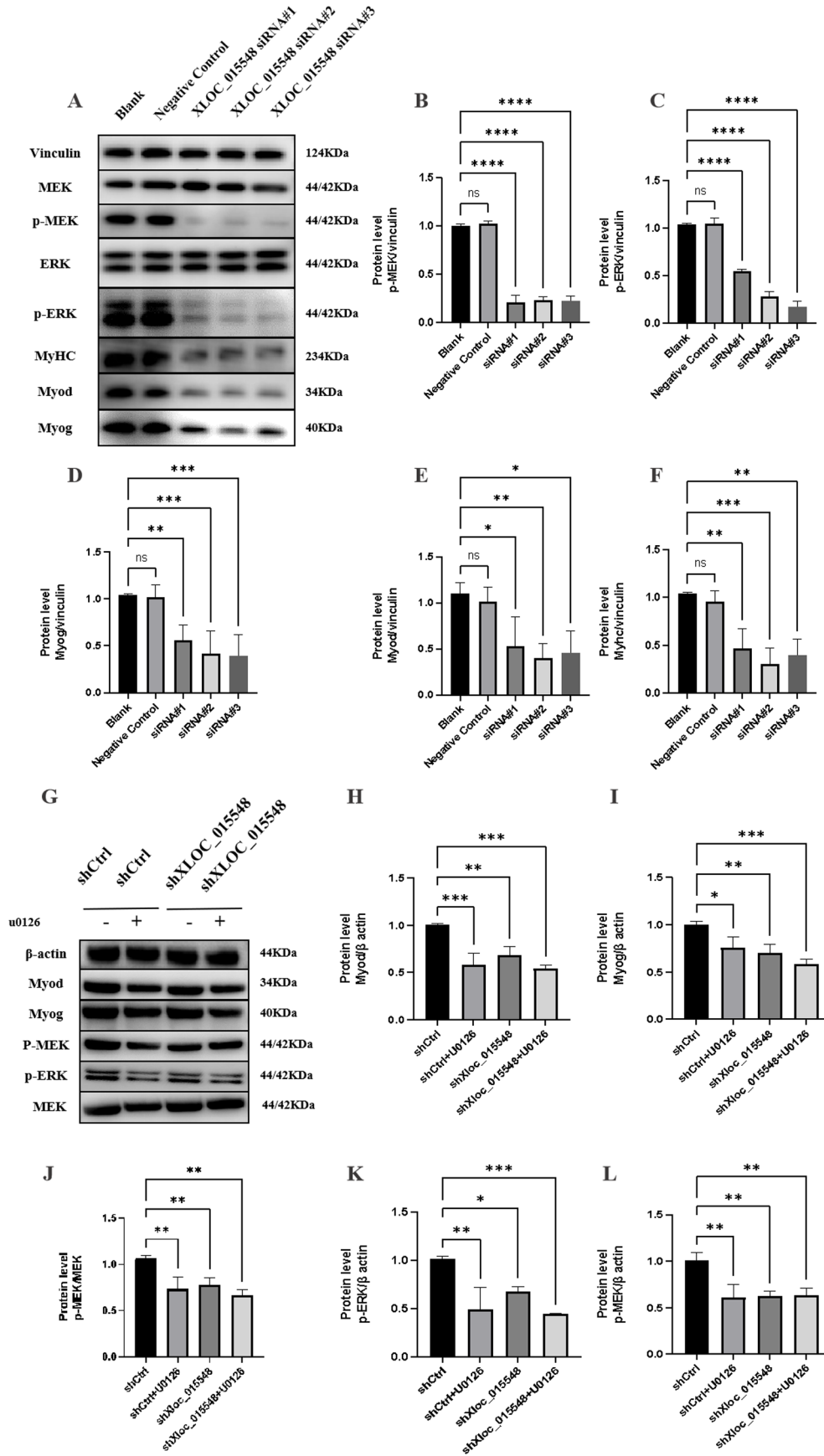


Figure 4. XLOC_015548 activated the MAPK/MEK/ERK signaling pathway and promoted myogenic differentiation. (A–F) The expression of phosphorylated proteins of MEK1/2 and ERK1/2 in the MAPK pathway and myoblast-related proteins were detected using western blot analysis in XLOC_015548-siRNA groups. (G–L) After treatment with 1 μ M U0126, the expression level of phosphorylated proteins of MEK/ERK or myogenic differentiation factors was detected using western blot analysis. Each experiment was repeated three times, and the data were expressed as mean \pm standard deviation. * P < 0.05; ** P < 0.01.

It is feasible to use this method to construct gene editing cell model.

XLOC_015548 also plays a positive regulatory role in cell morphology and differentiation. To test the role of XLOC_015548 in differentiation, we observed cell morphology and stimulated cell movement and contraction with carbachol. When cells were stimulated with carbachol, morphologically larger myotube cells showed stronger contractility. By comparing cell morphology and contractility index, XLOC_015548 promotes myoblastic differentiation and myocyte fusion, increases myotube activity, and enhances contractile exercise ability.

At present, it is believed that the regulation mechanism of cell fusion is mainly related to the adhesion molecules and membrane protein structures on the cell membrane, such as P4-ATPase flippase subunit CDC50A and L-type amino acid transporter 1 (LAT1).^{39–41} As one of the characteristics of skeletal myogenic differentiation, the fusion of individual myocytes into multinucleated mature myotubes has also been shown to be regulated by genetic mechanisms distinct from myogenic differentiation. Some studies have found that small open reading frames (sORF) exist in lncRNA, and the sORF-encoded micropeptide may be related to cell fusion.^{42,43} In XLOC_015548, which we explored, there was also a unrecognized sORF that had a base sequence coincidence with the gene encoding zonadhesin-like protein, encoding a conserved 46-amino-acid micropeptide (unpublished data). Therefore, exploring the mechanism of XLOC promoting myoblast fusion and whether XLOC has the ability to encode micropeptides that promote myoblast fusion is worth further exploration in the future.

To identify the specific mechanism of XLOC in myoblast differentiation, lentivirus-infected cells were further investigated in combination with MAPK/MEK pathway inhibitor U0126. As a MAPK/MEK inhibitor, U0126 can specifically inhibit MEK/ERK phosphorylation. Zhang *et al.*⁴⁴ also demonstrated that it could inhibit MEK/ERK phosphorylation in the MAPK pathway. Previous studies have shown that the MAPK signaling pathway is a key step in myogenesis, including ERK and P38, and its role in myogenesis has been extensively studied.^{45–48} Besides, various stimuli, such as inflammatory cytokines, tumor necrosis factors, and growth factors, can activate the MAPK pathway in satellite cells. In some studies, the inhibitors of the MAPK pathway are used to prevent the fusion of muscle cells into myotubes and the induction of muscle-specific genes,⁴⁹ whereas some constitutively active mutants, such as the ectopic expression of MKK6, can be forced to activate the MAPK signaling pathway, which would induce the expression of myocyte differentiation markers and the appearance of multinucleated myotubes.⁵⁰ When Myod induction is blocked by the absence of MAPK signaling in cells, proliferation would be stopped in satellite cells.⁵¹ The MAPK pathway plays a key role in the generation and differentiation of normal muscle cells, and the activation of this pathway can promote and accelerate the proliferation and differentiation of muscle cells.^{52,53}

Myod is a marker of early differentiation of myocytes, and Myog and MyHC are considered as markers of late differentiation. In this experiment, the expression levels of Myog and MyHC were decreased in the XLOC_015548

inhibition group, while the expression level of Myod was increased in the over-expression group. Therefore, we believe that XLOC_015548 may achieve its effect on myoblast differentiation at the early and late stages of differentiation. Skeletal muscle differentiation is a complex process involving different signaling pathways. In this study, we aimed to investigate whether XLOC_015548 could regulate the phosphorylation of MAPK signaling pathway-related proteins to positively affect the differentiation of myoblasts. We detected the MAPK pathway-related protein MEK/ERK. Combined with the results of pathway enrichment in KEGG database, XLOC_015548 showed a strong correlation with MAPK signaling pathway. It was observed that the degree of change of MAPK/MEK/ERK phosphorylation level was positively correlated with the level of cell differentiation. Therefore, we deduce that XLOC_015548 can positively regulate myoblast differentiation by mediating MAPK signaling pathway and regulating the phosphorylation degree of MEK/ERK.

In summary, an XLOC_015548 gene editing model was constructed in this study for the first time, and lentivirus technology was used to realize the knockdown or over-expression of key genes. The knockdown of XLOC_015548 could inhibit the proliferation and differentiation of myoblasts, thereby inhibiting the formation of myotubes and aggravating muscle atrophy. This experiment also has some limitations. We used LV-shRNA and LV-over-expression system, and there may be some biological compensation after long-term screening of puromycin. Therefore, in order to further explore the functional mechanism of XLOC_015548, we will further construct gene-edited mice and further elaborate them in *in vivo* experiments. As far as the present results are concerned, combining with previous RNA-seq results, it can be maintained that XLOC_015548 may promote myogenic differentiation through the MAPK signaling pathway and ultimately affect skeletal muscle atrophy. These findings provide a novel treatment idea for improving disuse muscle atrophy, including denervation-induced muscle atrophy. A potential mechanism for muscle atrophy injuries was also revealed. In conclusion, the findings provide a laboratory foundation for the clinical application of lncRNAs as regulatory factors in the treatment of disuse muscle atrophy.

AUTHORS' CONTRIBUTIONS

JW and HZ designed the study. TQ and YW performed the experiments. SC, FY, and WZ contributed to the analysis and collection of data. YW wrote the paper.

DECLARATION OF CONFLICTING INTERESTS

The author(s) declared no potential conflicts of interest with respect to the research, authorship, and/or publication of this article.

FUNDING

The author(s) disclosed receipt of the following financial support for the research, authorship, and/or publication of this article: This study was supported by National Natural Science Foundation of China (No. 82001319, 82172432, and 82102568),

National & Local Joint Engineering Research Center of Orthopaedic Biomaterials (no. XMHT20190204007), Shenzhen High-level Hospital Construction Fund, Shenzhen Key Medical Discipline Construction Fund (no. SZXK023), Shenzhen “San-Ming” Project of Medicine (no. SZSM201612092), and Guangdong Basic and Applied Basic Research Foundation (nos 2021A1515012586, 2019A1515011290, and 2019A1515110983).

ORCID ID

Yihao Wei  <https://orcid.org/0000-0002-7636-0294>

SUPPLEMENTAL MATERIAL

Supplemental material for this article is available online.

REFERENCES

- Lindholm ME, Giacomello S, Werne Solnestam B, Fischer H, Huss M, Kjellqvist S, Sundberg CJ. The impact of endurance training on human skeletal muscle memory, global isoform expression and novel transcripts. *PLoS Genet* 2016;**12**:1–24.e1006294
- Du J, Zhang P, Zhao X, He J, Xu Y, Zou Q, Luo J, Shen L, Gu H, Tang Q, Li M, Jiang Y, Tang G, Bai L, Li X, Wang J, Zhang S, Zhu L. MicroRNA-351-5p mediates skeletal myogenesis by directly targeting lactamase-β and is regulated by lnc-mg. *FASEB J* 2019;**33**:1911–26
- Bergmeister KD, Aman M, Muceli S, Vujaklija I, Manzano-Szalai K, Unger E, Byrne RA, Scheinecker C, Riedl O, Salminger S, Frommlet F, Borschel GH, Farina D, Aszmann OC. Peripheral nerve transfers change target muscle structure and function. *Sci Adv* 2019;**5**:1–10.eaau2956
- Cisterna BA, Vargas AA, Puebla C, Fernández P, Escamilla R, Lagos CF, Matus MF, Vilos C, Cea LA, Barnafi E, Gaete H, Escobar DF, Cardozo CP, Sáez JC. Active acetylcholine receptors prevent the atrophy of skeletal muscles and favor reinnervation. *Nat Commun* 2020; **11**:1–13
- Wang XH. MicroRNA in myogenesis and muscle atrophy. *Curr Opin Clin Nutr Metab Care* 2013;**16**:258–66
- MacLennan DH, Zvaritch E. Mechanistic models for muscle diseases and disorders originating in the sarcoplasmic reticulum. *Biochim Biophys Acta Mol Cell Res* 2011;**1813**:948–64
- Sun Z, Liu L, Liu N, Liu Y. Muscular response and adaptation to diabetes mellitus. *Front Biosci* 2008;**13**:4765–94
- Späte U, Schulze PC. Proinflammatory cytokines and skeletal muscle. *Curr Opin Clin Nutr Metab Care* 2004;**7**:265–9
- Kuang S, Kuroda K, Le Grand F, Rudnicki MA. Asymmetric self-renewal and commitment of satellite stem cells in muscle. *Cell* 2007;**129**:999–1010
- Zhang X, Chen M, Liu X, Zhang L, Ding X, Guo Y, Li X, Guo H. A novel lncRNA, lnc403, involved in bovine skeletal muscle myogenesis by mediating KRAS/Myf6. *Gene* 2020;**751**:1–10.e144706
- Yang Y, Yang J, Liu R, Li H, Luo X, Yang G. Accumulation of β-catenin by lithium chloride in porcine myoblast cultures accelerates cell differentiation. *Mol Biol Rep* 2011;**38**:2043–9
- Guo Y, Wang J, Zhu M, Zeng R, Xu Z, Li G, Zuo B. Identification of MyoD-responsive transcripts reveals a novel long noncoding RNA (lncRNA-AK143003) that negatively regulates myoblast differentiation. *Sci Rep* 2017;**7**:1–11
- Valdez MR, Richardson JA, Klein WH, Olson EN. Failure of Myf5 to support myogenic differentiation without myogenin, MyoD, and MRF4. *Dev Biol* 2000;**219**:287–98
- Lassar AB, Skapek SX, Novitch B. Regulatory mechanisms that coordinate skeletal muscle differentiation and cell cycle withdrawal. *Curr Opin Cell Biol* 1994;**6**:788–94
- Sabourin LA, Rudnicki MA. The molecular regulation of myogenesis. *Clin Genet* 2000;**57**:16–25
- Fatica A, Bozzoni I. Long noncoding RNAs: new players in cell differentiation and development. *Nat Rev Genet* 2014;**15**:7–21
- Derrien T, Johnson R, Bussotti G, Tanzer A, Djebali S, Tilgner H, Guernec G, Martin D, Merkel A, Knowles DG, Lagarde J, Veeravalli L, Ruan X, Ruan Y, Lassmann T, Carninci P, Brown JB, Lipovich L, Gonzalez JM, Thomas M, Davis CA, Shiekhattar R, Gingeras TR, Hubbard TJ, Notredame C, Harrow J, Guigó R. The GENCODE v7 catalog of human long noncoding RNAs: analysis of their gene structure, evolution, and expression. *Genome Res* 2012;**22**:1775–89
- Cesana M, Cacchiarelli D, Legnini I, Santini T, Sthandier O, Chinappi M, Tramontano A, Bozzoni I. A long noncoding RNA controls muscle differentiation by functioning as a competing endogenous RNA. *Cell* 2011;**147**:358–69
- Lu L, Sun K, Chen X, Zhao Y, Wang L, Zhou L, Sun H, Wang H. Genome-wide survey by ChIP-seq reveals YY1 regulation of lincRNAs in skeletal myogenesis. *EMBO J* 2013;**32**:2575–88
- Zhou L, Sun K, Zhao Y, Zhang S, Wang X, Li Y, Lu L, Chen X, Chen F, Bao X, Zhu X, Wang L, Tang LY, Esteban MA, Wang CC, Jauch R, Sun H, Wang H. Linc-YY1 promotes myogenic differentiation and muscle regeneration through an interaction with the transcription factor YY1. *Nat Commun* 2015;**6**:1–16
- Mueller AC, Cichewicz MA, Dey BK, Layer R, Reon BJ, Gagan JR, Dutta A. MUNC, a long noncoding RNA that facilitates the function of MyoD in skeletal myogenesis. *Mol Cell Biol* 2015;**35**:498–513
- Gong C, Li Z, Ramanujan K, Clay I, Zhang Y, Lemire-Brachat S, Glass DJ. A long noncoding RNA, lncMyoD, regulates skeletal muscle differentiation by blocking IMP2-mediated mRNA translation. *Developmental Cell* 2015;**34**:181–91
- Weng J, Zhang P, Yin X, Jiang B. The whole transcriptome involved in denervated muscle atrophy following peripheral nerve injury. *Front Mol Neurosci* 2018;**11**:69–15
- Boutros T, Chevet E, Metrakos P. Mitogen-activated protein (MAP) kinase/MAP kinase phosphatase regulation: roles in cell growth, death, and cancer. *Pharmacol Rev* 2008;**60**:261–310
- Peng WX, Huang JG, Yang L, Gong AH, Mo YY. Linc-RoR promotes MAPK/ERK signaling and confers estrogen-independent growth of breast cancer. *Mol Cancer* 2017;**16**:1–11
- Kuppasamy P, Soundharrajan I, Kim DH, Hwang I, Choi KC. 4-hydroxy-3-methoxy cinnamic acid accelerate myoblasts differentiation on C2C12 mouse skeletal muscle cells via AKT and ERK 1/2 activation. *Phytomedicine* 2019;**60**:152873–7
- Weng J, Wang YH, Li M, Zhang DY, Jiang BG. GSK3β inhibitor promotes myelination and mitigates muscle atrophy after peripheral nerve injury. *Neural Regen Res* 2018;**13**:324–30
- Dutt V, Gupta S, Dabur R, Injeti E, Mittal A. Skeletal muscle atrophy: potential therapeutic agents and their mechanisms of action. *Pharmacol Res* 2015;**99**:86–100
- Mitchell WK, Williams J, Atherton P, Larvin M, Lund J, Narici M. Sarcopenia, dynapenia, and the impact of advancing age on human skeletal muscle size and strength; a quantitative review. *Front Physiol* 2012;**3**:260–18
- Gordon BS, Kelleher AR, Kimball SR. Regulation of muscle protein synthesis and the effects of catabolic states. *Int J Biochem Cell Biol* 2013; **45**:2147–57
- Bonaldo P, Sandri M. Cellular and molecular mechanisms of muscle atrophy. *Dis Model Mech* 2013;**6**:25–39
- Schiaffino S, Dyar KA, Ciciliot S, Blaauw B, Sandri M. Mechanisms regulating skeletal muscle growth and atrophy. *FEBS J* 2013;**280**:4294–314
- Iwahashi S, Hashida R, Matsuse H, Higashi E, Bekki M, Iwanaga S, Hara K, Higuchi T, Hirakawa Y, Kubota A, Imagawa H, Muta Y, Minamitani K, Yoshida T, Yokosuka K, Yamada K, Sato K, Shiba N. The impact of sarcopenia on low back pain and quality of life in patients with osteoporosis. *BMC Musculoskelet Disord* 2022;**23**:142
- Li L, Du X, Ling H, Li Y, Wu X, Jin A, Yang M. Gene correlation network analysis to identify regulatory factors in sciatic nerve injury. *J Orthop Surg Res* 2021;**16**:1–19
- Navarro X. Functional evaluation of peripheral nerve regeneration and target reinnervation in animal models: a critical overview. *Euro J Neurosci* 2016;**43**:271–86
- Shen Y, Zhang R, Xu L, Wan Q, Zhu J, Gu J, Huang Z, Ma W, Shen M, Ding F, Sun H. Microarray analysis of gene expression provides new insights into denervation-induced skeletal muscle atrophy. *Front Physiol* 2019;**10**:1298–14

37. Wall BT, Dirks ML, Van Loon LJ. Skeletal muscle atrophy during short-term disuse: implications for age-related sarcopenia. *Ageing Res Rev* 2015;**12**:898–906
38. Zhu M, Liu J, Xiao J, Yang L, Cai M, Shen H, Chen X, Ma Y, Hu S, Wang Z, Hong A, Li Y, Sun Y, Wang X. Lnc-mg is a long noncoding RNA that promotes myogenesis. *Nat Commun* 2017;**8**:1–11
39. Millay DP. Regulation of the myoblast fusion reaction for muscle development, regeneration, and adaptations. *Exp Cell Res* 2022;**2**:113–34
40. Grifell-Junyent M, Baum JF, Välimets S, Herrmann A, Paulusma CC, López-Marqués RL, Günther Pomorski T. CDC50A is required for aminophospholipid transport and cell fusion in mouse C2C12 myoblasts. *J Cell Sci* 2022;**5**:1–11
41. Collao N, Akohene-Mensah P, Nallabelli J, Binet ER, Askarian A, Lloyd J, Niemi GM, Beals JW, van Vliet S, Rajgara R, Saleh A, Wiper-Bergeron N, Paluska SA, Burd NA, De Lisio M. The role of L-type amino acid transporter 1 (Slc7a5) during in vitro myogenesis. *Am J Physiol Cell Physiol* 2022;**2**:C595–605
42. Anderson DM, Anderson KM, Chang CL, Makarewich CA, Nelson BR, McAnally JR, Kasaragod P, Shelton JM, Liou J, Bassel-Duby R, Olson EN. A micropeptide encoded by a putative long noncoding RNA regulates muscle performance. *Cell* 2015;**160**:595–606
43. Nelson BR, Makarewich CA, Anderson DM, Winders BR, Troupes CD, Wu F, Reese AL, McAnally JR, Chen X, Kavalali ET, Cannon SC, Houser SR, Bassel-Duby R, Olson EN. A peptide encoded by a transcript annotated as long noncoding RNA enhances SERCA activity in muscle. *Science* 2016;**351**:271–6
44. Zhang F, Yan T, Guo W, Sun K, Wang S, Bao X, Liu K, Zheng B, Zhang H, Ren T. Novel oncogene COPS3 interacts with Beclin1 and Raf-1 to regulate metastasis of osteosarcoma through autophagy. *J Exp Clin Cancer Res* 2018;**37**:1–12
45. Liu S, Gao F, Wen L, Ouyang M, Wang Y, Wang Q, Luo L, Jian Z. Osteocalcin induces proliferation via positive activation of the PI3K/Akt, P38 MAPK pathways and promotes differentiation through activation of the GPRC6A-ERK1/2 pathway in C2C12 myoblast cells. *Cell Physiol Biochem* 2017;**43**:1100–12
46. Cai Q, Wu G, Zhu M, Xue C, Cheng B, Xu S, Wu P. FGF6 enhances muscle regeneration after nerve injury by relying on ERK1/2 mechanism. *Life Sci* 2020;**248**:1–12
47. Segalés J, Perdiguero E, Muñoz-Cánoves P. Regulation of muscle stem cell functions: a focus on the p38 MAPK signaling pathway. *Front Cell Dev Biol* 2016;**4**:91–15
48. Choi CH, Lee BH, Ahn SG, Oh SH. Proteasome inhibition-induced p38 MAPK/ERK signaling regulates autophagy and apoptosis through the dual phosphorylation of glycogen synthase kinase 3 β . *Biochem Biophys Res Commun* 2012;**418**:759–64
49. Charville GW, Cheung TH, Yoo B, Santos PJ, Lee GK, Shrager JB, Rando TA. Ex vivo expansion and in vivo self-renewal of human muscle stem cells. *Stem Cell Rep* 2015;**5**:621–32
50. Lluís F, Perdiguero E, Nebreda AR, Muñoz-Cánoves P. Regulation of skeletal muscle gene expression by p38 MAP kinases. *Trends Cell Biol* 2006;**16**:36–44
51. Troy A, Cadwallader AB, Fedorov Y, Tyner K, Tanaka KK, Olwin BB. Coordination of satellite cell activation and self-renewal by Par-complex-dependent asymmetric activation of p38 α / β MAPK. *Cell Stem Cell* 2012;**11**:541–53
52. Di Vona C, Bezdán D, Islam AB, Salichs E, López-Bigas N, Ossowski S, de la Luna S. Chromatin-wide profiling of DYRK1A reveals a role as a gene-specific RNA polymerase II CTD kinase. *Molecular Cell* 2015;**57**:506–20
53. Tiwari VK, Stadler MB, Wirbelauer C, Paro R, Schübeler D, Beisel C. A chromatin-modifying function of JNK during stem cell differentiation. *Nature Genetics* 2012;**44**:94–100

(Received July 7, 2022, Accepted December 11, 2022)